Toxicology and Applied Pharmacology 305 (2016) 66–74

Contents lists available at ScienceDirect

Toxicology and Applied Pharmacology

journal homepage: www.elsevier.com/locate/ytaap

Assessment of ABCG2-mediated transport of pesticides across the rabbit placenta barrier using a novel MDCKII in vitro model

Sandra Halwachs [a], Ingo Schäfer [b], Carsten Kneuer [c], Peter Seibel [b], Walther Honscha [a,*]

[a] Institute of Pharmacology, Pharmacy and Toxicology, Faculty of Veterinary Medicine, Universität Leipzig, Leipzig, Germany
[b] Molecular Cell Therapy, Center for Biotechnology and Biomedicine, Faculty of Medicine, Universität Leipzig, Leipzig, Germany
[c] Federal Institute for Risk Assessment (BfR), Pesticide Safety, Max-Dohrn-Straße 8-10, D-10589 Berlin, Germany

ARTICLE INFO

Article history:
Received 2 March 2016
Revised 3 May 2016
Accepted 7 June 2016
Available online 08 June 2016

Keywords:
Placenta
ABCG2 (BCRP)
Transport
Rabbit
Developmental toxicity
Pesticides

ABSTRACT

In humans, the ATP-binding cassette efflux transporter ABCG2 contributes to the fetoprotective barrier function of the placenta, potentially limiting the toxicity of transporter substrates to the fetus. During testing of chemicals including pesticides, developmental toxicity studies are performed in rabbit. Despite its toxicological relevance, ABCG2-mediated transport of pesticides in rabbit placenta has not been yet elucidated. We therefore generated polarized MDCK II cells expressing the ABCG2 transporter from rabbit placenta (rbABCG2) and evaluated interaction of the efflux transporter with selected insecticides, fungicides, and herbicides. The Hoechst H33342 accumulation assay indicated that 13 widely used pesticidal active substances including azoxystrobin, carbendazim, chlorpyrifos, chlormequat, diflufenican, dimethoate, dimethomorph, dithianon, ioxynil, methiocarb, propamocarb, rimsulfuron and toclofos-methyl may be rbABCG2 inhibitors and/or substrates. No such evidence was obtained for chlorpyrifos-methyl, epoxiconazole, glyphosate, imazalil and thiacloprid. Moreover, chlorpyrifos (CPF), dimethomorph, tolclofos-methyl and rimsulfuron showed concentration-dependent inhibition of H33342 excretion in rbABCG2-transduced MDCKII cells. To further evaluate the role of rbABCG2 in pesticide transport across the placenta barrier, we generated polarized MDCKII-rbABCG2 monolayers. Confocal microscopy confirmed correct localization of rbABCG2 protein in the apical plasma membrane. In transepithelial flux studies, we showed the time-dependent preferential basolateral to apical (B > A) directed transport of [^{14}C] CPF across polarized MDCKII-rbABCG2 monolayers which was significantly inhibited by the ABCG2 inhibitor fumitremorgin C (FTC). Using this novel in vitro cell culture model, we altogether showed functional secretory activity of the ABCG2 transporter from rabbit placenta and identified several pesticides like the insecticide CPF as potential rbABCG2 substrates.

1. Introduction

Pesticides are used in conventional agriculture to manage weeds, insects or fungi while non-agricultural pesticides (biocides) have a wider range of applications as disinfectants, preservatives, and in pest control. Consumers are continuously exposed to pesticides mainly through residues in the diet (Hamilton et al., 2004). In addition, users and bystanders can be directly exposed during pesticide and biocide application. However, recent human biomonitoring suggests that consumer exposure to agricultural pesticides is mostly through dietary sources even for residents living near agricultural land (Galea et al., 2015). Because of their inherent activity and toxicity, chronic pesticide exposure is considered as a potential public health risk specifically to susceptible sub-populations such as pregnant women and their fetuses. From the mechanistic perspective, developmental toxicity in the fetus resulting from maternal pesticide exposure can occur, among others, through endocrine disruption, placenta or neuronal cell defects, and oxidative stress (Ewence et al., 2015; Mostafalou and Abdollahi, 2013; Saulsbury et al., 2008). Thus, depending on the underlying mechanism, maternofetal transfer of the active substance can be essential for developmental toxicity.

Generally, during gestation the placenta serves as a protective barrier to fetal exposure of potentially harmful compounds like pesticides. Interestingly, the ATP-binding cassette (ABC) efflux transporter ABCG2 is highly expressed in human syncytiotrophoblast cells (Allikmets et al., 1998) that form the placenta barrier between the maternal and the fetal blood circulations. Therefore, ABCG2 was initially named ABCP (ABC transporter in placenta) (Allikmets et al., 1998). The efflux

Abbreviations: ABCG2, ATP-binding cassette sub-family G member 2; CPF, chlorpyrifos; DAPI, 4′-6-diamidino-2-phenylindole; FTC, fumitremorgin C; MDCKII, Madin-Darby canine kidney type II cells; MRL, maximum residue limits; P_{app}, apparent permeability coefficient; TEER, transepithelial electrical resistance; ZO-1, Tight junction protein 1.

* Corresponding author at: Institute of Pharmacology, Pharmacy and Toxicology, Faculty of Veterinary Medicine, Universität Leipzig, Leipzig, Germany.
E-mail address: honscha@vetmed.uni-leipzig.de (W. Honscha).

http://dx.doi.org/10.1016/j.taap.2016.06.007

transporter is also known as breast cancer resistance protein (BCRP) or multixenobiotic resistance (MXR) transporter due to its initial isolation from multidrug-resistant breast cancer MCF-7 (Doyle et al., 1998) or mitoxantrone-resistant colon carcinoma cells (Miyake et al., 1999). In syncytiotrophoblast cells, ABCG2 is localized in the apical plasma membrane facing the maternal side and mediates cellular excretion of various drugs and toxins (Vähäkangas and Myllynen, 2009; Lindner et al., 2013). Hence, ABCG2 substantially contributes to the protective barrier function of the placenta by limiting the placental penetration and thereby fetal exposure to potential harmful xenobiotics (Robey et al., 2009). However, no detailed information is so far available on active transport of pesticides including ABCG2 in the placenta barrier.

Due to similar hemomonochorial morphology and placenta function (Fischer et al., 2012), the rabbit is the preferred non-rodent species to test the prenatal developmental toxicity of chemicals including pesticides in human (OECD, 2011). Accordingly, developmental toxicity studies in rabbits are included in legislative data requirements for pesticides (e.g. Regulation (EU) No. 283/2013). We have recently cloned the ABCG2 transporter from placenta tissues of a chinchilla rabbit that was subsequently referred to as rabbit ABCG2 (rbABCG2). Using MDCKII cells stably expressing rbABCG2, we demonstrated functional efflux activity of the ABCG2 transporter from rabbit placenta (Halwachs et al., 2016). Moreover, rbABCG2 was shown to interact with several drugs that are known human ABCG2 substrates indicating a comparable drug substrate specificity of the rbABCG2 and the human ABCG2 efflux transporter supporting the choice of the rabbit as a model for developmental toxicity testing of chemicals. However, there is no information so far available on the role of rbABCG2 in placental transport and fetal disposition with potential harmful environmental chemicals like pesticides.

In this study, we therefore aimed to explore the MDCKII-rbABCG2 cell line as in vitro model to test active transport of pesticides in rabbit placenta. In a first step, a range of herbicides, fungicides, and insecticides were screened for interaction with rbABCG2 using the Hoechst H33342 assay. Only those active substances were included that are approved in the EU (Lewis et al., 2015), repeatedly exceeded the legal maximum residue levels (MRLs) in food monitoring studies (BVL reports, 2013) or were considered of high environmental significance due to combined extensive use in agriculture and inherent toxicological hazard (Schmidt and Gutsche, 2000). We further established functional monolayers of polarized MDCKII-rbABCG2 cells. In subsequent transport studies including transepithelial flux studies, we examined functional rbABCG2 secretory activity and evaluated selected pesticides like the organophosphorus insecticide chlorpyrifos as potential rbABCG2 substrates.

2. Materials and methods

2.1. Chemicals

Bisbenzimide Hoechst H33342 was purchased from AppliChem (Darmstadt, Germany). Methiocarb was obtained from Dr. Ehrenstorfer Inc. (Augsburg, Germany) and all other substances including all tested pesticides were purchased from Sigma-Aldrich (Deisenhofen, Germany) at analytical grade (Table 1). Mouse monoclonal anti-ABCG2 antibody BXP-21 was obtained from Calbiochem (Darmstadt, Germany) and polyclonal anti-ZO-1 (TJP-1) antibody from Sigma-Aldrich. Secondary antibodies were from Invitrogen (Darmstadt, Germany).

2.2. Cell culture

Madin-Darby canine kidney (MDCKII) cells stably expressing ABCG2 from rabbit placenta (rbABCG2) including culture conditions of MDCKII-rbABCG2 and parental MDCKII cells (wild type, WT) were described recently (Halwachs et al., 2016). Cells (1×10^4 per well) were seeded on Polyester Transwell®-Clear inserts (0.33 cm^2 growth area, 0.4 μm pore size, Corning, Wiesbaden, Germany) and cultured to polarized monolayers using 0.3 and 0.7 ml culture medium for the inner and outer chamber, respectively. Formation of barrier function was followed by measurement of the transepithelial electrical resistance (TEER) using a low-impedance volt-ohm meter equipped with a Chopstick electrode (Millipore, Schwalbach, Germany).

2.3. Cell proliferation assay

We evaluated the short-term (4 h) cytotoxicity of all tested pesticides using the WST-1 (4-[3-(4-iodophenyl)-2-(4-nitrophenyl)-2H-5-tetrazolio]-1,3-benzene disulfonate) cytotoxicity assay (Roche Applied

Table 1
The selected pesticides chemicals were obtained at analytical grade from Sigma-Aldrich (Deisenhofen, Germany) with the specified purity as provided in the table and stock solutions were prepared with specified solvents. In this study, the applied pesticide concentrations (highlighted in grey) reflected the MRL in cereals or vegetables. MRL values were taken from the EU pesticides data base available at: http://ec.europa.eu/food/plant/pesticides/eu-pesticides-database/public/?event=activesubstance.selection&language=EN (last access: 12/18/2015). Here, the respective higher pesticide MRL was used and cells were incubated with the respective 0.1- or one-fold MRL concentration.

No.	Pesticide	Substance group	Solvent	Maximum MRL (mg/kg)	Maximum MRL (mg/kg)	Lot/batch-no	Specified purity	Solvent
				cereals [molar concentration]	vegetables [molar concentration]			[concentration]
1	Azoxystrobin	Strobilurin	Toluene	0.30 [744.00 nM]	15.00 [37.18 μM]	SZBB130XV	99.40%	0.10%
2	Carbendazim	Benzimidazole	DMF	2.00 [10.50 μM]	0.10 [523.00 nM]	SZBA347XV	99.20%	0.04%
3	Chlormequat-chloride	Quarternary ammonium	Milli Q	2.00 [12.65 μM]	0,05 [316.00 nM]	SZB8248XV	99.1%	0.10%
3	Chlorpyrifos	Organophosphate	Toluene	0.02 [57.00 nM]	1.00 [2.85 μM]	SZBA141XV	99.90%	0.10%
4	Chlorpyrifos-methyl	Organophosphate	Toluene	3.00 [9.30 μM]	0.50 [1.55 μM]	SZBC109XV	99.90%	0.25%
5	Diflufenican	Carboxamide	Methanol	0.01 [25.00 nM]	0.05 [127.00 nM]	SZBC048XV	97.90%	0.10%
6	Dimethoate	Organophosphate	Methanol	0.01 [44.00 nM]	0.02 [87.00 nM]	SZBC243XV	99.50%	0.04%
7	Dimethomorph	Morpholine	Methanol	0.05 [129.00 nM]	15.00 [38.67 μM]	SZB9069XV	99.00%	0.02%
8	Dithianon	Quinone	Toluene	0.05 [169.00 nM]	0.60 [2.02 μM]	SZBA327XV	97.40%	0.10%
9	Epoxiconazole	Thiazole	Toluene	1.50 [4.55 μM]	0.10 [303.00 nM]	SZBD099XV	99.00%	0.10%
10	Glyphosate	Phosphonate	Milli Q	10.00 [59.50 μM]	0.50 [2.97 μM]	SZBC164XV	99.90%	0.04%
11	Imazalil	Imidazole	Toluene	0.05 [168.00 nM]	3.00 [10.09 μM]	SZB9016XV	99.70%	0.10%
12	Ioxynil	Hydroxybenzonitrile	Methanol	0.05 [135.00 nM]	3.00 [8.09 μM]	SZB8114XV	99.80%	0.15%
13	Methiocarb	Carbamate	Xylene	0.10 [444.00 nM]	1.00 [4.44 μM]	10,630	99,5%	0,10%
14	Propamocarb	Carbamate	Methanol	0.10 [531.00 nM]	50.00 [265.50 μM]	SZB9168XV	99.3%	0.10%
15	Rimsulfuron	Sulfonylurea	Ethyl-acetate	0.05 [116.00 nM]	0.05 [115.00 nM]	SZBC047XV	99.90%	0.05%
16	Thiacloprid	Neonicotinoid	Ethyl-acetate	1.00 [3.96 μM]	5.00 [19.79 μM]	SZBC180XV	99.90%	0.10%
17	Tolclofos-methyl	Chlorophenyl	Methanol	0.05 [166.00 nM]	2.00 [6.64 μM]	SZBA323XV	97.90%	0.20%

Science, Mannheim, Germany) as described previously (Halwachs et al., 2007). The IC_{50} values of the selected compounds were defined as the substance concentration that reduced the absorbance by 50% and were determined using Prism 5.04 (GraphPad Software Inc., San Diego, CA).

2.4. Immunocytochemical analysis

For indirect immunolocalization of ABCG2, MDCKII-rbABCG2 or -WT cells were grown on microporous filter inserts for 5 days. Polarized cell monolayers were fixed with 2% (v/v) paraformaldehyde and unspecific binding was blocked with 3% (v/v) BSA in phosphate-buffered saline. We detected ABCG2 protein with *anti*-ABCG2 MAb (BXP-21; 1:50) overnight at 4 °C followed by incubation with goat *anti*-mouse Alexa 594 IgG (1:500) for 2 h at room temperature. Tight-junction-associated zona occludens 1 (ZO-1) protein was detected using polyclonal *anti*-ZO-1 antibody (TJP-1; 1:100) overnight at 4 °C and stained with goat anti-rabbit Alexa 488 IgG (1:400) for 2 h at room temperature. Cell nuclei were visualized using 4′,6-diamidino-2-phenylindole (DAPI; 0.5 μg/ml). Samples were mounted on slides with FluorSave reagent (Calbiochem). Confocal images (x-z plane) of MDCKII-rbABCG2 or -WT cells were taken by sequential scanning of optical sections of about 0.17 μm thickness as defined recently (Wassermann et al., 2014b) on an inverted confocal laser scanning microscope Leica TCS SP5 equipped with an HCX PL APO 63 × 1.4 oil immersion objective (Leica Microsystems, Wetzlar, Germany). Image stacks were processed and analysed with LAS AF1.7.0 software (Leica Microsystems) and Adobe Photoshop CS2.

2.5. Hoechst H33342 accumulation assays in MDCKII-rbABCG2 and MDCKII-WT cells

MDCKII-rbABCG2 or -WT cells were seeded (8×10^3) in 96-well culture plates and grown to confluence. Monolayers were incubated for 4 h with the pesticides specified in Table 1. Pesticide stock solutions were prepared using the solvents delineated in Table 1 and vehicle concentrations were ≤0.25% for all experiments. In the absence of suitable biomonitoring data on pesticide levels in human plasma, tested concentrations were based on maximum residue limits (MRL) in cereals or vegetables and included levels corresponding to 0.01, 0.1 or 10-fold the MRL. Following equilibration with the pesticide, we incubated the cells with the fluorescent dye Hoechst H33342 (20 μM) for 15 min as described recently (Wassermann et al., 2013a). Protein concentration of cells was determined using the bicinchoninic acid (BCA) assay (Pierce, Rockford, IL, USA) according to the manufacturer's instructions. The intracellular H33342 accumulation was assessed as relative fluorescence units (RFU) per mg protein in relation to untreated control cells. Finally, the functional rbABCG2 efflux activity was defined as the ratio in H33342 accumulation of MDCKII-rbABCG2 cells compared to that found in MDCKII-WT control cells.

2.6. Transepithelial chlorpyrifos transport studies

MDCKII-rbABCG2 or -WT cells were grown on microporous membrane filters as delineated above. Flux studies were conducted in 5 day-old cell cultures (Wassermann et al., 2013b). Before the start of the transport assays, culture medium was replaced by medium with or without FTC (10 μM). After 2 h, MDCKII monolayers were washed with Hank's balanced salt solution (HBSS, PAA) supplemented with 20 mM glucose and 20 mM hydroxyethylpiperazineethane sulfonic acid (HEPES; pH 7.8). Transport experiments were initiated by addition of HBSS transport buffer containing 10 μM [^{14}C] chlorpyrifos (CPF; 6.6×10^5 dpm/ml; specific activity: 1.11×10^3 MBq/mmol; purity: 99%; lot number: 140,718; Biotrend, Cologne, Germany) with or without 10 μM FTC to either the apical (for determination of apical to basolateral transport, A > B) or the basolateral (for determination of basolateral to apical transport, B > A) compartment. Aliquots (10 μl) from the apical (for determination of basolateral to apical transport, B > A) or the basolateral (for determination of apical to basolateral transport, A > B) compartment were taken and replaced by fresh transport buffer at 30, 60, 120, 180 and 240 min. Radioactivity of samples was measured by liquid scintillation counting (LS 6500, Beckman, Fullerton, CA). Total cellular protein was determined by BCA assay and CPF transport across MDCKII monolayers was expressed in pmol per mg protein. The apparent permeability coefficient (P_{app}) was calculated using the following equation: P_{app} [cm/s] = flux [pmol/h]/3600 [s/h]/S[pmol/cm^3]/0,33 [cm^2] where S defines the initial substrate concentration. The efflux ratio (ER) represents the ratio of the P_{app} in the basolateral-to-apical direction (P_{app} B > A) to the P_{app} in the apical-to-basolateral direction (P_{app} A > B).

Following each flux assay, MDCKII monolayer barrier function was confirmed by measuring the paracellular flux of Lucifer yellow (LY) added at 60 μM to the apical compartment over 1 h at 37 °C. LY levels were assessed in aliquots (10 μl) from the apical or the basolateral compartment using a fluorescence microplate reader (480/530 nm, Tecan, Crailsheim, Germany).

2.7. Statistics

Analysis of data was carried out using Microsoft Excel software (Office 2010). Curve fittings for the transepithelial CPF flux were performed by nonlinear regression by means of SigmaPlot 10 (Systat Software Inc.) We assessed differences between mean values of MDCKII-rbABCG2 and -WT cells as well as differences between pretreated MDCKII cultures compared to untreated control cells by two-way ANOVA and the Fisher LSD as post hoc test using SigmaPlot 10. A p-value of <0.05 was considered as statistically significant.

3. Results

3.1. Effect of selected pesticides on Hoechst H33342 accumulation in MDCKII-rbABCG2 or MDCKII-WT cells

Before initiation of Hoechst H33342 transport assays, acute cytotoxicity of the chosen pesticides in MDCKII-rbABCG2 cultures was determined by the WST-1 assay. Dimethomorph significantly reduced WST-1 conversion at a concentration of 39 μM, corresponding to the maximum MRL in vegetables (not shown). Therefore, concentrations of 0.01, 0.13, 1.3 and 13 μM, were used in subsequent studies with dimethomorph. An IC_{50}-value of ~11 mM was obtained for the fungicide propamocarb. For all other tested pesticides, IC_{50}-values could not be obtained as cell viability remained >50% of vehicle control after short-term incubation (4 h) with the highest applied concentration of azoxystrobin (1860 μM), carbendazim (525 μM), chlorpyrifos (285 μM), chlorpyrifos-methyl (31 μM), chlormequate chloride (1260 μM), diflufenican (13 μM), dimethoate (22 μM), dimethomorph (26 μM), dithianon (202 μM), epoxiconazole (455 μM), glyphosate (148 μM), imazalil (109 μM), ioxynil (540 μM), methiocarb (440 μM), rimsulfuron (12 μM), thiacloprid (396 μM) and tolclofos-methyl (17 μM).

The effect of 18 selected pesticides on accumulation of the ABCG2 model substrate Hoechst H33342 (Hegedus et al., 2009) in MDCKII-rbABCG2 cells was tested to identify potential ABCG2 substrates and/or inhibitors. Substrates as well as inhibitors can be identified in the indirect Hoechst screening assay through their inhibition of cellular H33342 excretion (Wassermann et al., 2013a), resulting in elevated intracellular H33342 levels. Unspecific effects on substrate accumulation were taken into account by normalization to H33342 accumulation in MDCKII-WT cells. Overall, 13 pesticides showed inhibition of H33342 excretion in MDCKII-rbABCG2 cells but not in MDCKII-WT control cells at the selected maximum concentrations. This is illustrated by the 1.5- to 2-fold significant increase in the cellular H33342

accumulation rbABCG2 to WT ratio compared to the untreated control shown in Fig. 1. Among these 13 pesticides, lower concentrations of chlorpyrifos and dimethomorph (Fig. 1A) as well as rimsulfuron and tolclofos-methyl (Fig. 1B) corresponding to one tenth of the reference MRL also showed an inhibitory effect on H33342 excretion comparable to that of the higher concentration (Fig. 1). Altogether, the screening level assay identified 13 of 18 selected pesticidal active substances as potential rbABCG2 substrates and/or inhibitors.

3.2. Concentration-dependent effect of selected pesticides on H33342 excretion in MDCKII-rbABCG2 and -WT cells

In subsequent studies, we examined the concentration-dependency of the effect of chlorpyrifos, dimethomorph, rimsulfuron, and tolclofos-methyl on cellular H33342 accumulation in more detail. As described in the materials and methods section, test concentrations were selected on basis of the highest available MRL, corresponding to 0.03–28.5 μM chlorpyrifos, 0.01–13 μM dimethomorph, 1.16–1160 nM rimsulfuron and 0.07–66.4 μM tolclofos-methyl. For all four substances, a concentration-dependent increase in the H33342 accumulation rbABCG2 to WT ratio was observed (Fig. 2). The lowest concentration of chlorpyrifos (Fig. 2A), dimethomorph (Fig. 2B), rimsulfuron (Fig. 2C) or tolclofos-methyl (Fig. 2D) did not cause any statistically significant elevation of cellular H33342 levels. At the next concentration level, intracellular H33342 was significantly increased for all substances. For rimsulfuron (Fig. 2C) and tolclofos-methyl (Fig. 2D) there was no significant further increase ín H33342 accumulation when comparing the 3rd and 4th concentration level. This was not the case for chlorpyrifos (Fig. 2A) and dimethomorph (Fig. 2B), where the highest concentration level was associated with a further significant increase in cellular H33342 levels. Altogether, our results demonstrated a concentration dependency of effect of chlorpyrifos, dimethomorph, rimsulfuron, and tolclofos-methyl on H33342 accumulation in MDCK-rbABCG2 cells.

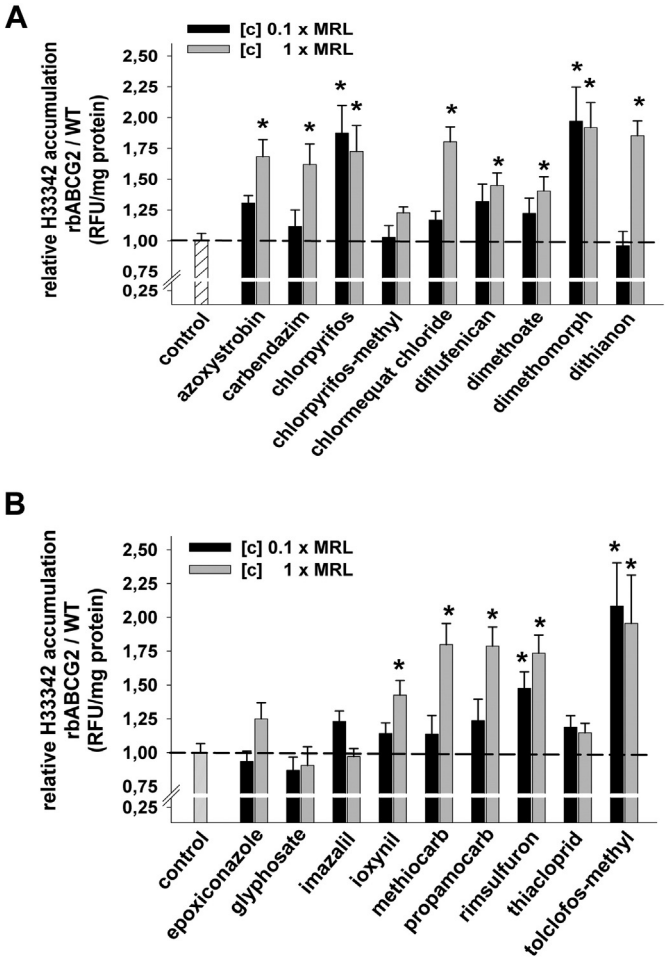

Fig. 1. Impact of selected pesticides on Hoechst H33342 accumulation in MDCKII-rbABCG2 or MDCKII-WT cells. Cells were pre-treated (4 h) with the pesticides azoxystrobin, carbendazim, chlormequat chloride, chlorpyrifos, chlorpyrifos-methyl, diflufenican, dimethoate, dimethomorph or dithianon (A) and the pesticides epoxiconazole, glyphosate, imazalil, ioxynil, methiocarb, propamocarb, rimsulfuron, thiacloprid or tolclofos-methyl (B). Pesticide concentrations reflected the 0.1- or one-fold MRL in cereals or vegetables as specified in Table 1. In case of dimethomorph, we used the one- or ten-fold MRL in cereals as stated in the results section. Hoechst assays were initiated by addition of H33342 (10 μM) in presence or absence of the respective pesticide and cells were incubated for 15 min. Cellular H33342 accumulation was assessed as delineated in the Materials and methods Section. ABCG2 efflux activity was defined as the ratio in H33342 accumulation in the rbABCG2 clone compared to that determined in MDCKII-WT cells and expressed as RFU per mg protein. Data represent the mean ± SEM (*$p < 0.05$ significance to untreated control cells, two-way ANOVA, Fisher LSD post hoc test, $n = 18$).

3.3. Formation of a functional MDCKII cell monolayer

Epithelial barrier characteristics of polarized MDCKII-rbABCG2 or MDCKII-WT cell monolayers are pre-requisite for Transwell-based flux studies and were thus monitored by TEER measurements. Cell cultures reached confluence within three days after seeding on membrane filters involving a steep increase in TEER values to 126.0 ± 2.2 Ohm × cm2 (not shown). The following stationary culture phase was generally associated with a drop of TEER values to a plateau level over a maximum culture period of six days (not shown). In 5 day-old cultures, we measured TEER values of 64 ± 4 Ω × cm^2 in MDCKII-rbABCG2 cells and of 76 ± 2 Ω × cm^2 in MDCKII-WT cells. Formation of functional MDCKII monolayers was further assessed by immunostaining of the TJ-associated protein ZO-1. As shown in Fig. 3, ZO-1 protein was localized by confocal microscopy at the apical and lateral side between adjacent cells in both cell lines.

Integrity of the MDCKII monolayer barrier was additionally monitored after each flux assay by measuring the permeability of the transcellular flux marker LY (Irvine et al., 1999). In this study, we determined a mean P_{app} value for LY of 3.55 ± 0.73 × 10^{-6} cm/s across MDCKII-rbABCG2 monolayers. In MDCKII-WT cells, the mean LY P_{app} value was 5.42 ± 1.01 × 10^{-6} cm/s. In regard to the initial LY concentration added, the paracellular LY permeability across MDCKII monolayers was <1% in all experiments.

3.4. Subcellular localization of rbABCG2 in polarized MDCKII monolayers

To determine the subcellular distribution of the ABCG2 protein from rabbit placenta (rbABCG2) in MDCKII-rbABCG2, cells were cultured on microporous filter inserts. Five day-old immunostained polarized monolayers were examined via X–Z sectioning by confocal microscopy. As shown in Fig. 3A, rabbit ABCG2 was detected at the apical plasma membrane and apical parts of the lateral membrane. There, it localized in proximity to ZO-1 protein. In MDCKII-WT cells, only a weak and mostly diffuse ABCG2 signal was observed (Fig. 3B).

3.5. Transepithelial transport of chlorpyrifos

In order to elucidate the involvement of ABCG2 in active pesticide transport in the rabbit placental barrier, we representatively examined transepithelial transport of the insecticide chlorpyrifos (CPF) across MDCKII-rbABCG2 and -WT monolayers. The flux studies were performed in 5 day-old polarized monolayers. The epithelial barrier function was monitored by TEER measurements and paracellular LY permeability.

Initially, time-dependent vectorial transport of [^{14}C] CPF (10 μM) was determined. The apically (B > A) directed or the basolaterally directed (A > B) pesticide transport was calculated as the flux of [^{14}C] CPF into the receiver compartment. In regard to B > A directed CPF

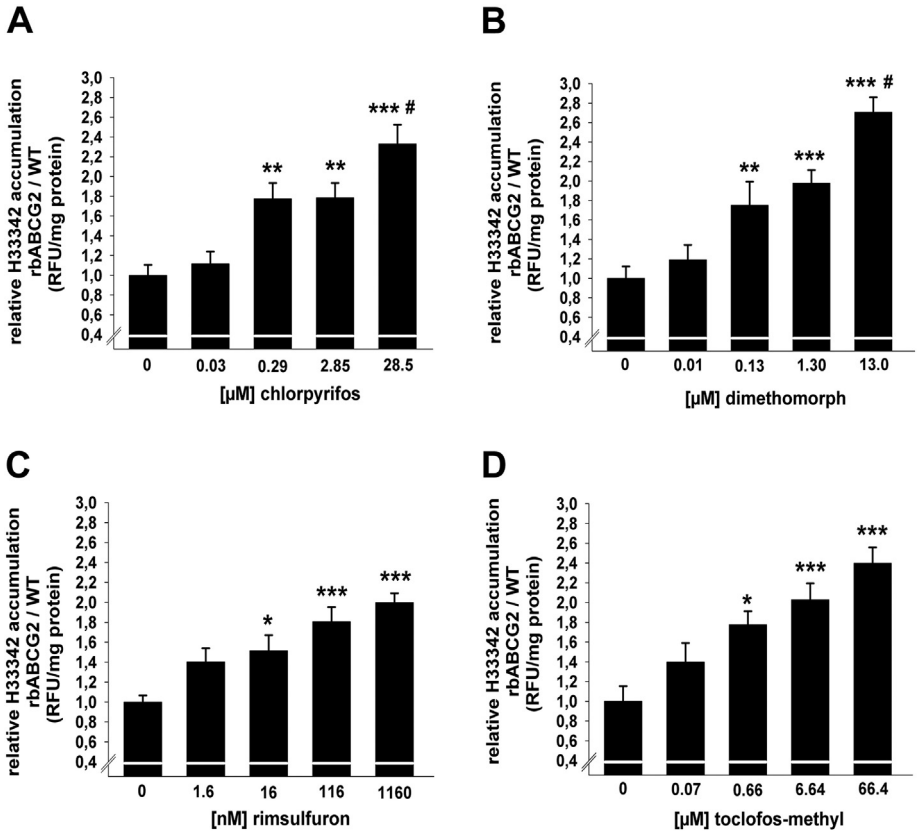

Fig. 2. Concentration-dependent effect of selected pesticides on Hoechst H33342 accumulation in MDCKII-rbABCG2 or MDCKII-WT cells. Cells were pre-treated (4 h) with different concentrations of the pesticides chlorpyrifos (A), dimethomorph (B), rimsulfuron (C) or tolclofos-methyl (D). Pesticide concentrations reflected the 0.01-, 0.1-, one- or ten-fold MRL in cereals or vegetables as specified in Table 1. Cellular H33342 accumulation and ABCG2 efflux activity was determined as described in the figure legend of Fig. 1. Values are mean ± SEM (* $p < 0.05$, ** $p < 0.01$, *** $p < 0.001$ to vehicle control, Fig. 2A: # $p < 0.05$ to 2.85 µM CPF, Fig. 2B # $p < 0.05$ to 1.3 µM dimethomorph, two-way ANOVA, Fisher LSD post hoc test, $n = 12$).

transport, an uptake phase over up to 120 min was generally observed in MDCKII-rbABCG2 and in MDCKII-WT cells (Fig. 4). This uptake phase was followed by an equilibrium plateau phase in both cell lines. Compared to the WT control, we observed a significantly higher [^{14}C] CPF B > A flux in rbABCG2-transduced MDCKII cells (Fig. 4). In this study, only a slight time-dependent basolaterally directed (A > B) pesticide flux was detected which did not significantly differ between the cell lines (Fig. 4).

Addition of the specific ABCG2 inhibitor FTC (10 µM) (Rabindran et al., 2000) resulted in a significant reduction of the B > A directed [^{14}C] CPF flux in MDCKII-rbABCG2 cells (Fig. 5A) to the level of the WT control (Fig. 5B). In the MDCKII-WT cell line, FTC had no relevant effect on CPF flux (Fig. 5B). In both cell lines, the time-dependent A > B directed [^{14}C] CPF flux was not significantly altered by FTC (Fig. 5). To further characterize efflux activity of rabbit ABCG2, we calculated P_{app} values for the B > A and A > B flux of [^{14}C] CPF within the initial phase (120 min) in MDCKII-bABCG2 and MDCKII-WT cells. As shown in Fig. 6, CPF showed a preferential transepithelial B > A flux across polarized monolayers of both cell lines. In rbABCG2-transduced MDCKII cells, the B > A P_{app} values were significantly higher than in MDCKII-WT cells. The ABCG2 inhibitor FTC caused a significant decrease in [^{14}C] CPF P_{app} values in MDCKII-rbABCG2 (Fig. 6A) but not in -WT cells (Fig. 6B). In both cell lines, P_{app} values for the basolateral (A > B) directed CPF flux were not significantly altered by FTC in relation to untreated control cells (Fig. 6). Concordantly, significantly higher transepithelial CPF flux ratios (B > A/A > B) were observed in MDCKII-rbABCG2 (4.52 ± 0.12) compared to WT cells (2.80 ± 0.04) (Fig. 6C). In relation to the untreated control, FTC caused a significant decrease in CPF flux ratios in rbABCG2-transduced cells to the level of MDCKII-WT control cells (2.90 ± 0.04) (Fig. 6C). In contrast, the ABCG2 inhibitor FTC had no relevant effect on the flux ratio of CPF in MDCKII-WT monolayers (2.83 ± 0.05) (Fig. 6C).

4. Discussion

In the first part of this study, we screened 18 widely used pesticidal active substances including insecticides, fungicides or herbicides for interaction with the ABC-transporter ABCG2 from rabbit placenta (rbABCG2) (Halwachs et al., 2016). Various approaches can be followed when selecting appropriate concentrations. Ideally, concentrations tested in vitro would reflect measured levels in blood or target tissue. Unfortunately, such information is rarely available for pesticides. Published biomonitoring studies at best report the urinary excretion of metabolites or other biomarkers (Galea et al., 2015). Another common approach is to test the highest attainable concentrations, usually determined either by solubility limits or cytotoxicity in the assay system. However, positive outcomes in such a setting are likely to be unrelated to the situation at "realistic" concentrations and may thus be misleading when it comes to the selection of candidates for follow-up. Therefore, we chose pesticide concentrations based on the maximum residue limit (MRL) in vegetables or cereals. MRLs are set based on knowledge about the actual agricultural practice, the resulting residue level as well as the mammalian toxicity. Consumers including pregnant women may regularly be exposed to pesticide residues through the diet specifically through consumption of vegetables that are frequently consumed raw or semi-processed. Therefore, vegetables are expected to contain high pesticides residues compared to other food groups (MAFF, 2000), although detected levels usually remain below the MRL (EFSA, European Food Safety Authority, 2013). With exception of 40 µM dimethomorph, none of the 18 tested pesticides exhibited

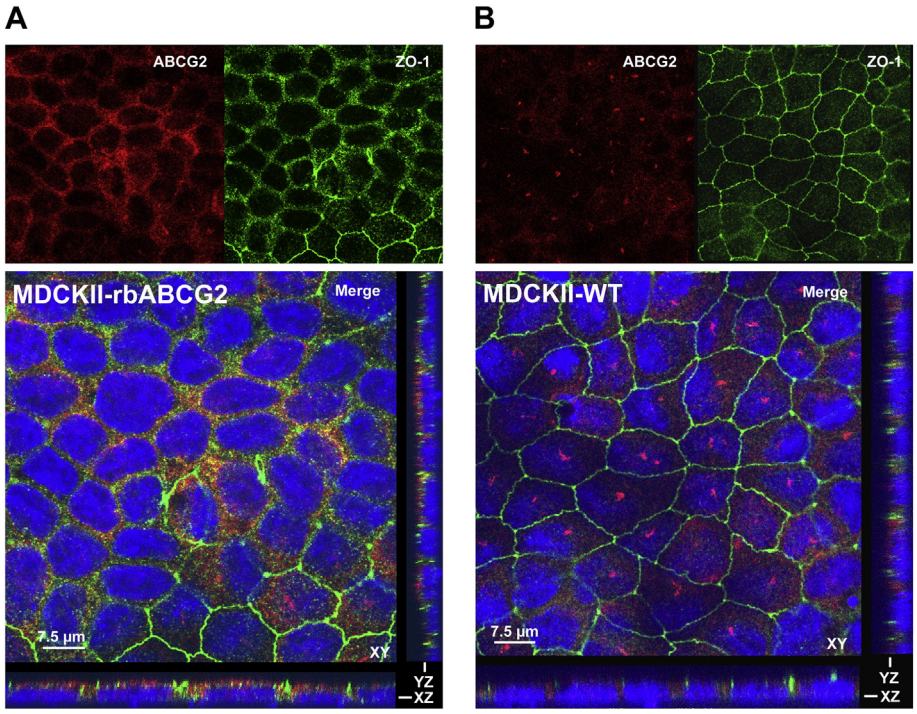

Fig. 3. Subcellular localization of ABCG2 and detection of ZO-1 in MDCKII-rbABCG2 cells. 5 day-old polarized MDCKII-bABCG2 (A) or MDCKII-WT (B) cell monolayers were fixed and stained for rabbit ABCG2 and ZO-1. Cell nuclei (*blue*) were visualized using DAPI. Optical XY sectioning with the corresponding XZ- or YZ-section was performed by confocal laser scanning microscopy (A and B). ABCG2 protein (*red*) was localized at the apical surface of MDCKII-rbABCG2 cells where ABCG2 co-localized with tight junction protein ZO-1 (*green*). In the WT control, a faint ABCG2 signal was observed mainly in the lateral membrane adjacent to MDCKII-WT cells (B). Control incubations included omission of primary antibody. Representative cells are shown from two independent experiments.

acute cytotoxicity in MDCKII-rbABCG2 cells at concentrations up to 10 times the MRL for vegetables or cereals. Interestingly, in dimethomorph toxicity studies the dog was the most sensitive species with a converted no observed adverse effect level (NOAEL) of ~12 μM based on hepatocellular alterations in the 1-yr study (EFSA, European Food Safety Authority, 2006). In all subsequent studies non-toxic concentrations of dimethomorph were used.

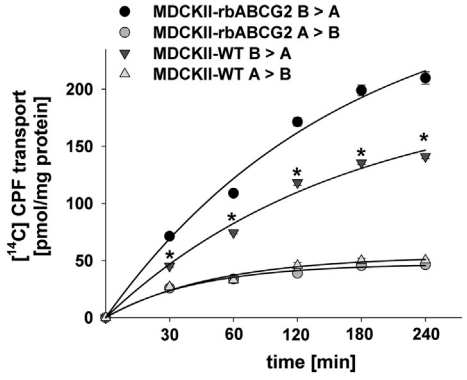

Fig. 4. Time-dependent transepithelial transport of chlorpyrifos across MDCKII-bABCG2 and MDCKII-WT monolayers. Polarized MDCKII monolayers were obtained by culture on porous membrane filters for 5 days. Transport experiments were initiated by addition of 10 μM [^{14}C] chlorpyrifos (CPF) in the respective compartment and aliquots were taken at 30, 60, 120, 180, and 240 min as described in the Material and Methods section. Vectorial [^{14}C] CPF transport across MDCKII monolayers was determined as the apically directed B > A or the basolaterally directed A > B flux of CPF. Radioactivity was measured by liquid scintillation counting and CPF transport was expressed in pmol per mg protein. Values are mean ± SEM (*$p < 0.05$ significantly different to B > A flux of [^{14}C] CPF in rbABCG2-transduced MDCKII cells; two-way ANOVA, Fisher LSD post-hoc test; data are shown from six monolayers with each $n = 3$ as technical replicates).

The screening identified 13 of 18 substances of diverse chemical structure as inhibitors or substrates of rbABCG2 in the Hoechst H33342 assay. Similarly, earlier studies demonstrated interaction of ABC efflux transporter P-glycoprotein (P-gp) with structural diverse pesticides (Bain and LeBlanc, 1996; Georgantzopoulou et al., 2014; Leslie et al., 2005). Interestingly, chlorpyrifos (CPF) increased H33342 excretion in MDCKI-rbABCG2 cells at concentrations of 2.85 and 0.285 μM, but chlorpyrifos-methyl did not when tested at higher concentrations of 9.3 and 0.93 μM. Hence, our results indicate that CPF but not chlorpyrifos-methyl interact with rbABCG2. Both substances have similar physico-chemical properties (Lewis et al., 2015) but while CPF represents a diethyl-organophospoester, chlorpyrifos-methyl corresponds to the respective dimethyl-ester. Likewise, an absence of a relation between lipophilicity and potential for pesticide-transporter interaction was reported for the P-gp efflux transporter (Pivčević and Zaja, 2006; Georgantzopoulou et al., 2014). For the insecticide CPF as well as the fungicides dimethomorph and tolclofos-methyl and the herbicide rimsulfuron, we performed additional assays to investigate the concentration-response relationship. A clearly concentration-dependent increase H33342 accumulation in MDCKII-rbABCG2 cells for all four substance provides confirmatory evidence for an interaction with rbABCG2.

In evaluation of rbABCG2-pesticide interactions in MDCKII cells, intrinsic H33342-transporting efflux transporters as canine ABCG2 or canine P-gp have to be taken into account (Kneuer et al., 2007). However, we did not detect a relevant alteration in H33342 accumulation in MDCKII-WT control cells by the tested pesticides. Moreover, we recently showed that the *P*-gp inhibitor verapamil did not block the initial (20 min) H33342 efflux in MDCKII-rbABCG2 cells (Halwachs et al., 2016). Therefore, H33342 excretion in MDCKII-rbABCG2 cells can be clearly attributed to functional rbABCG2 efflux activity. Altogether, our results suggested the pesticidal active substances CPF, dimethomorph,

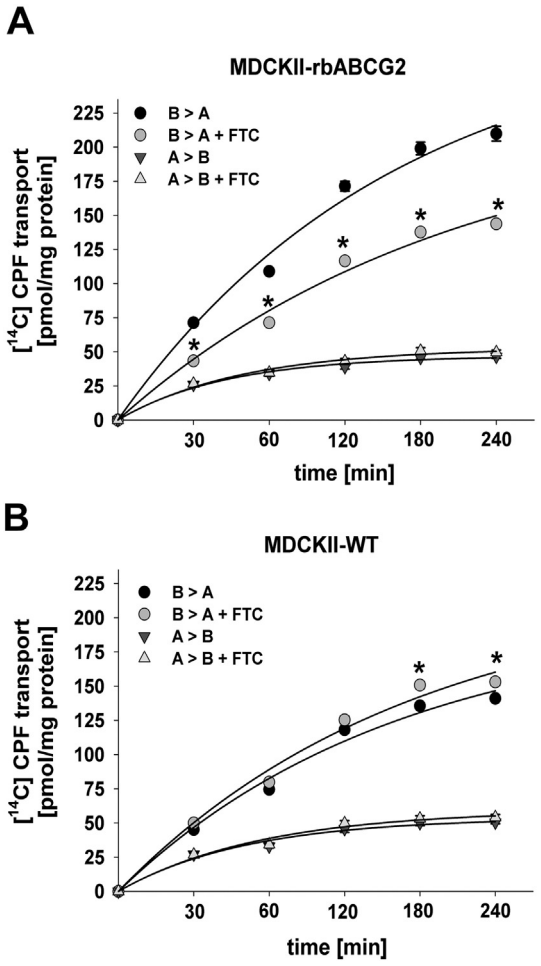

Fig. 5. Effect of FTC on time-dependent vectorial transport of chlorpyrifos in MDCKII-rbABCG2 cells. We pre-treated 5 day-old polarized MDCKII-bABCG2 (A) or MDCKII-WT (B) cell monolayers with FTC (10 μM) for 2 h. Then, transport experiments were initiated by addition of [^{14}C] CPF (10 μM) in the respective donor compartment and time-dependent vectorial CPF transport was measured in the absence or presence of FTC as delineated in the figure legend of Fig. 4. The results represent the mean ± SEM (*$p < 0.05$ significantly different to B > A flux of [^{14}C] CPF in rbABCG2-transduced MDCKII cells; two-way ANOVA, Fisher LSD post-hoc test; data are shown from six monolayers with each $n = 3$ as technical replicates).

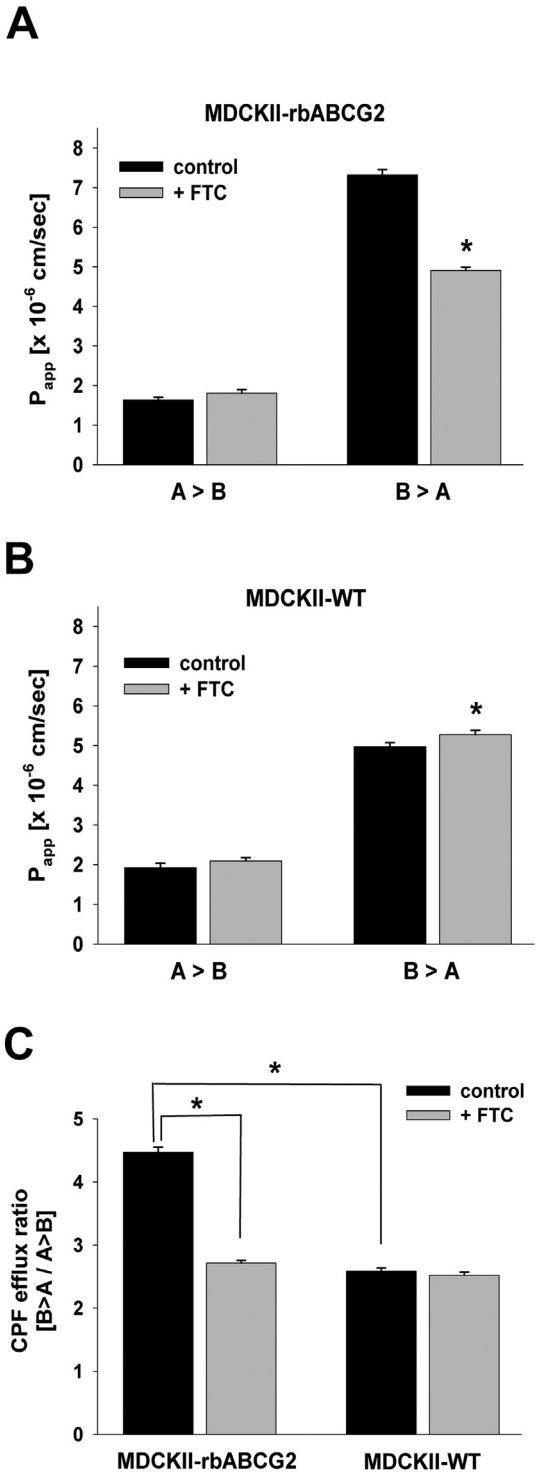

Fig. 6. Impact of FTC on CPF flux in MDCKII-rbABCG2 or MDCKII-WT cells. Polarized MDCKII monolayers were pre-incubated with FTC (10 μM) for 2 h. Then, [^{14}C] CPF (10 μM) transport was determined as described in the figure legend of Fig. 5. P_{app} values for CPF in MDCKII-rbABCG2 (A) or -WT (B) cells as well as CPF efflux ratios (C) in the absence or presence of FTC in both cell lines were calculated as described in the Material and methods section. Values are mean ± SD (*$p < 0.05$ significantly different to untreated control cells, two-way ANOVA, Fisher LSD post-hoc test; data are shown from six monolayers with each $n = 3$ as technical replicates).

tolclofos-methyl, and rimsulfuron as substrates and/or inhibitors of rbABCG2-mediated transport.

Nevertheless, the Hoechst screening assay is an indirect setup and therefore does not clearly distinguish between rbABCG2 substrates and inhibitors (Hegedus et al., 2009). Hence, in the second part of this study we performed representative transepithelial transport studies using [^{14}C]-labeled CPF as potential rbABCG2 substrate. For this purpose, we generated polarized MDCKII-rbABCG2 monolayers as in vitro placenta barrier model. The placenta represents an epithelial barrier composed of tight-junctioned syncytiotrophoblast cells exhibiting ABCG2 expression in the apical plasma membrane (Vähäkangas and Myllynen, 2009; Lindner et al., 2013). In agreement with these reports, we detected rbABCG2 efflux transporter in the apical surface of the MDCKII-rbABCG2 monolayer model. In five-day old MDCKII-rbABCG2 cultures, obtained TEER values were in the same range of ~100 $\Omega \times cm^2$ formerly reported for functional MDCKII monolayers in the stationary culture phase (Irvine et al., 1999; Wassermann et al., 2013b). Furthermore, the average P_{app} value of the paracellular flux marker Lucifer yellow (LY) corresponded with the previously reported LY permeability in MDCK monolayers with P_{app} values of $\leq 5 \times 10^{-6}$ cm/s (Irvine et al., 1999). Moreover, we detected tight-junction (TJ)-associated zona occludens 1 (ZO-1) protein between adjacent MDCKII-rbABCG2 cells suggesting a direct involvement of this TJ protein in cell barrier formation. Likewise, in normal human placentae of first and third trimester gestation, ZO-1 was localized in the apical part of the syncytium, in cell–cell contacts between syncytium and villous cytotrophoblastic cells as well as between the latter (Marzioni et al., 2001). Hence, our

results demonstrated epithelial barrier characteristics of our MDCKII-rbABCG2 cell culture model comparable to the placenta epithelial barrier.

To examine carrier-mediated placental transport in vitro, human primary cytotrophoblasts or human choriocarcinoma BeWo, JEG-3 or JAR cells have been used as model of the trophoblast layer. Primary cytotrophoblasts, JEG-3 and JAR cells are generally not suggested as sufficient barrier models for transepithelial flux studies (Prouillac and Lecoeur, 2010). BeWO cells are able to form tight-junctioned monolayers on semipermeable membrane inserts. However, the barrier function significantly varies among different BeWo clones and cell culture conditions (Prouillac and Lecoeur, 2010). In contrast, standardized experimental conditions for transepithelial transport studies in MDCK cells exist (Braun et al., 2000). Moreover, MDCK cells express several ABC multidrug efflux transporters similar to placenta tissue or BeWO cells (Prouillac and Lecoeur, 2010). Genbacev et al. (2011) published a protocol describing the isolation of proliferating progenitor trophoblast cells and the generation of differentiated trophoblasts from these cells. The later may provide an interesting model to study transplacental transport in an environment more closely related to the in vivo situation than the MDCK and other in vitro models. However, for the purposes described here, we considered the polarized MDCKII-rbABCG2 monolayers as adequate to screen for substances potentially undergoing active ABCG2-mediated transport across epithelial barriers like rabbit placenta.

In agreement with apical membrane localization of rbABCG2, we observed a preferential apically directed saturable transport of the organophosphorus insecticide CPF across polarized MDCKII-rbABCG2 monolayers. This high net CPF efflux was illustrated by a CPF efflux ratio (B > A/A > B) of ~4.5. Moreover, in rbABCG2-transduced MDCKII cells the ABCG2 inhibitor FTC significantly reduced the CPF efflux ratio to the level of MDCKII-WT cells. Thus, our results demonstrated specific rbABCG2-mediated CPF transport. MDCKII-WT also showed apically directed CPF transport with an efflux ratio of ~2 suggesting involvement of intrinsic ABC efflux pumps (Giacomini et al., 2010) in CPF transport across MDCKII-rbABCG2 monolayers. However, FTC did not significantly alter the CPF efflux ratio in MDCKII-WT cells. Thus, relevant contribution of canine ABCG2 to CPF transport is unlikely. Data on the role of other ABC transporters in CPF efflux is rare and heterogeneous. Previous inhibition studies indicated interaction of CPF with P-gp (Bain and LeBlanc, 1996). However, in this study P-gp-transduced murine melanoma cells lacked actual P-gp-mediated CPF transport. Besides, results from competitive binding studies suggested that the active CPF metabolite chlorpyrifos oxon but not the parent substance CPF interacts with P-gp (Lanning et al., 1996). Overall, a significant role of P-gp in CPF transport seems not likely. However, we cannot exclude the general involvement of other endogenously expressed ABC transporters (Kneuer et al., 2007) like multidrug-resistance associated proteins (MRPs) in the CPF efflux in our MDCKII cell culture model.

One of the substances that did not show any indication for inhibition of rbABCG2 in this study was glyphosate, a widely used herbicide. The tested concentrations of 6 and 60 μM cover the range that can be expected in plasma based on biomonitoring data for urine from exposed farmers and their families (Acquavella et al., 2004). In the ex-vivo perfused placenta model, low transplacental passage has been shown for this highly hydrophilic substance and was quantified as 15% under the specific experimental conditions (Mose et al., 2008). This was confirmed in a comparative in vitro study in BeWO cells (Poulsen et al., 2009). Our results suggest, that the limited materno-fetal transfer was not due to a potential active ABCG2-mediated extrusion in the opposite direction, but other (presumably physicochemical) restriction. Thus, for glyphosate unlike for chlorpyrifos, toxicokinetic interactions at the placental ABCG2 which may increase fetal exposures would not be expected.

In conclusion, this is the first report on functional secretory activity of the ABCG2 transporter cloned from rabbit placenta (rbABCG2). Our results altogether indicate that 13 widely used pesticidal active substances including azoxystrobin, carbendazim, chlorpyrifos, chlormequat, diflufenican, dimethoate, dimethomorph, dithianon, ioxynil, methiocarb, propamocarb, rimsulfuron and toclofos-methyl may be rbABCG2 inhibitors and/or substrates. No such evidence was obtained for chlorpyrifos-methyl, epoxiconazole, glyphosate, imazalil and thiacloprid. For chlorpyrifos, dimethomorph, rimsulfuron and toclofos-methyl, concentration-dependency of the effect was described, confirming the initial finding. In addition, Transwell flux studies showed that chlorpyrifos is a rbABCG2 substrate. Maternal exposure to the insecticide chlorpyrifos causes developmental toxicity including intrauterine growth retardation and neurotoxicity in laboratory animals (Muto et al., 1992). Besides, chlorpyrifos induced apoptosis of human placental cells that may also negatively impact fetal development (Saulsbury et al., 2008). In this study, we detected rbABCG2 interactions with chlorpyrifos concentrations similar to reported residue levels in food (EFSA, European Food Safety Authority, 2013). The in vivo relevance of our data is further corroborated by the increase in placental ABCG2 protein levels during gestation while expression of the other broad efflux pump P-gp significantly decreased with gestational age (Mathias et al., 2005). Hence, this study indicates that physiological rbABCG2 efflux activity in the placenta barrier plays an important role in fetal protection from pesticide-induced toxicity by limiting exposure to ABCG2 pesticide substrates in maternal circulation. Therefore, our results may overall help to understand the toxic effects of actively transported pesticides. Moreover, the MDCKII-rbABCG2 cell line may serve as a tool for in vitro screening and mechanistic studies in the context of developmental toxicity testing.

Conflict of interests

The authors declare that they have no conflict of interests.

Transparency document

The Transparency document associated with this article can be found, in online version.

Acknowledgements

We thank Birte Scholz and Cathleen Lakoma for skillful technical assistance. Funding was provided by the Federal Institute for Risk Assessment (BfR) (grant no. 1322-417 and 1329-427).

References

Acquavella, J.F., Alexander, B.H., Mandel, J.S., Gustin, C., Baker, B., Chapman, P., Bleeke, M., 2004. Glyphosate biomonitoring for farmers and their families: results from the Farm Family Exposure Study. Environ Health Perspect. 112 (3), 321–326.

Allikmets, R., Schriml, L.M., Hutchinson, A., Romano-Spica, V., Dean, M., 1998. A human placenta-specific ATP-binding cassette gene (ABCP) on chromosome 4q22 that is involved in multidrug resistance. Cancer Res. 58, 5337–5339.

Bain, L.J., LeBlanc, G.A., 1996. Interaction of structurally diverse pesticides with the human MDR1 gene product P-glycoprotein. Toxicol. Appl. Pharmacol. 141, 288–298.

Braun, A., Hämmerle, S., Suda, K., Rothen-Rutishauser, B., Günthert, M., Krämer, S.D., Wunderli-Allenspach, H., 2000. Cell cultures as tools in biopharmacy. Eur. J. Pharm. Sci. 11, S51–S60.

BVL reports [in German], 2013. Food Safety Report 2011. Monitoring. Joint report by the Federal Government and the Federal States. The Federal Office of Consumer Protection and Food Safety (BVL). BVL Reports 7, Springer, Basel, pp. 1–95. Available at: http://www.bvl.bund.de/DE/08_PresseInfothek/04_Publikationen/03_Berichte/infothek_berichte_node.html.

Doyle, L.A., Yang, W., Abruzzo, L.V., Krogmann, T., Gao, Y., Rishi, A.K., Ross, D.D., 1998. A multidrug resistance transporter from human MCF-7 breast cancer cells. Proc. Natl. Acad. Sci. U. S. A. 95, 15665–15670.

EFSA (European Food Safety Authority), 2006. Conclusion regarding the peer review of the pesticide risk assessment of the active substance dimethomorph. EFSA J. (doi: 10.2903/j.efsa.2006.82r. 69 pp. Available at:) www.efsa.europa.eu/efsajournal.

EFSA (European Food Safety Authority), 2013. The 2010 European Union report on pesticide residues in food. EFSA J. 11, 3130, doi:http://dx.doi.org/10.2903/j.efsa.2013.3130. (Available at:) www.efsa.europa.eu/efsajournal

Ewence, A., Brescia, S., Johnson, I., Rumsby, P.C., 2015. An approach to the identification and regulation of endocrine disrupting pesticides. Food Chem. Toxicol. 78, 214–220.
Fischer, B., Chavatte-Palmer, P., Viebahn, C., Navarrete Santos, A., Duranthon, V., 2012. Rabbit as a reproductive model for human health. Reproduction 144, 1–10.
Genbacev, O., Donne, M., Kapidzic, M., Gormley, M., Lamb, J., Gilmore, J., Larocque, N., Goldfien, G., Zdravkovic, T., McMaster, M.T., Fisher, S.J., 2011. Establishment of human trophoblast progenitor cell lines from the chorion. Stem Cells 29 (9), 1427–1436.
Georgantzopoulou, A., Skoczyńska, E., Van den Berg, J.H., Brand, W., Legay, S., Klein, S.G., Rietjens, I.M., Murk, A.J., 2014. P-gp efflux pump inhibition potential of common environmental contaminants determined in vitro. Environ. Toxicol. Chem. 33, 804–813.
Giacomini, K.M., Huang, S.M., Tweedie, D.J., Benet, L.Z., Brouwer, K.L., Chu, X., Dahlin, A., Evers, R., Fischer, V., Hillgren, K.M., Hoffmaster, K.A., Ishikawa, T., Keppler, D., Kim, R.B., Lee, C.A., Niemi, M., Polli, J.W., Sugiyama, Y., Swaan, P.W., Ware, J.A., Wright, S.H., Yee, S.W., Zamek-Gliszczynski, M.J., Zhang, L., International Transporter Consortium, 2010. Membrane transporters in drug development. Nat. Rev. Drug Discov. 9, 215–236.
Halwachs, S., Kneuer, C., Gohlsch, K., Müller, M., Ritz, V., Honscha, W., 2016. Generation of a novel in vitro-cell culture model to study active carrier-mediated transport of chemicals in the rabbit placenta. Placenta 38, 8–15. http://dx.doi.org/10.1016/j.placenta.2015.12.005 (Available at:).
Hamilton, D., Ambrus, Á., Dieterle, R., Felsot, A., Harris, C., Petersen, B., Racke, K., Wong, S.S., Gonzalez, R., Tanaka, K., Earl, M., Roberts, G., Bhula, R., 2004. Pesticide residues in food—acute dietary exposure. Pest Manag. Sci. 60, 311–339.
Hegedus, C., Szakacs, G., Homolya, L., Orban, T.I., Telbisz, A., Jani, M., 2009. Ins and outs of the ABCG2 multidrug transporter: an update on in vitro functional assays. Adv. Drug Deliv. Rev. 61, 47–56.
Irvine, J.D., Takahashi, L., Lockhart, K., Cheong, J., Tolan, J.W., Selick, H.E., Grove, J.R., 1999. MDCK (Madin-Darby canine kidney) cells: a tool for membrane permeability screening. J. Pharm. Sci. 88, 28–33.
Kneuer, C., Honscha, W., Gäbel, G., Honscha, K.U., 2007. Adaptive response to increased bile acids: induction of MDR1 gene expression and P-glycoprotein activity in renal epithelial cells. Pflugers Arch. 454, 587–594.
Lanning, C.L., Fine, R.L., Sachs, C.W., Rao, U.S., Corcoran, J.J., Abou-Donia, M.B., 1996. Chlorpyrifos oxon interacts with the mammalian multidrug resistance protein, P-glycoprotein. J. Toxicol. Environ. Health 47, 395–407.
Leslie, E.M., Deeley, R.G., Cole, S.P., 2005. Multidrug resistance proteins: role of P-glycoprotein, MRP1, MRP2, and BCRP (ABCG2) in tissue defense. Toxicol. Appl. Pharmacol. 204, 216–237.
Lewis, K.A., Green, A., Tzilivakis, J., Warner, D., 2015. The Pesticide Properties DataBase (PPDB) Developed by the Agriculture & Environment Research Unit (AERU), University of Hertfordshire, 2006–2015.
Lindner, S., Halwachs, S., Wassermann, L., Honscha, W., 2013. Expression and subcellular localization of efflux transporter ABCG2/BCRP in important tissue barriers of lactating dairy cows, sheep and goats. J. Vet. Pharmacol. Ther. 36, 562–570.
Marzioni, D., Banita, M., Felici, A., Paradinas, F.J., Newlands, E., De Nictolis, M., Mühlhauser, J., Castellucci, M., 2001. Expression of ZO-1 and occludin in normal human placenta and in hydatidiform moles. Mol. Hum. Reprod. 7, 279–285.
Mathias, A.A., Hitti, J., Unadkat, J.D., 2005. P-glycoprotein and breast cancer resistance protein expression in human placentae of various gestational ages. Am. J. Physiol. Regul. Integr. Comp. Physiol. 289, R963–R969.
Miyake, K., Mickley, L., Litman, T., Zhan, Z., Robey, R., Cristensen, B., Brangi, M., Greenberger, L., Dean, M., Fojo, T., Bates, S.E., 1999. Molecular cloning of cDNAs which are highly overexpressed in mitoxantrone-resistant cells: demonstration of homology to ABC transport genes. Cancer Res. 59, 8–13.
Mose, T., Kjaerstad, M.B., Mathiesen, L., Nielsen, J.B., Edelfors, S., Knudsen, L.E., 2008. Placental passage of benzoic acid, caffeine, and glyphosate in an ex vivo human perfusion system. J. Toxicol. Environ. Health A 71 (15), 984–991.
Mostafalou, S., Abdollahi, M., 2013. Pesticides and human chronic diseases: evidences, mechanisms, and perspectives. Toxicol. Appl. Pharmacol. 268, 157–177.
Muto, M.A., Lobelle Jr., F., Bidanset, J.H., Wurpel, J.N., 1992. Embryotoxicity and neurotoxicity in rats associated with prenatal exposure to DURSBAN. Vet. Hum. Toxicol. 34, 498–501.
OECD, 2011. OECD Guideline for the Testing of Chemicals No. 414: Prenatal Developmental Toxicity Study.
Pivčević, B., Zaja, R., 2006. Pesticides and their binary combinations as P-glycoprotein inhibitors in NIH 3T3/MDR1 cells. Environ. Toxicol. Pharmacol. 22, 268–276.
Poulsen, M.S., Rytting, E., Mose, T., Knudsen, L.E., 2009. Modeling placental transport: correlation of in vitro BeWo cell permeability and ex vivo human placental perfusion. Toxicol. in Vitro 23 (7), 1380–1386.
Prouillac, C., Lecoeur, S., 2010. The role of the placenta in fetal exposure to xenobiotics: importance of membrane transporters and human models for transfer studies. Drug Metab. Dispos. 38, 1623–1635.
Robey, R.W., To, K.K., Polgar, O., Dohse, M., Fetsch, P., Dean, M., Bates, S.E., 2009. ABCG2: a perspective. Adv. Drug Deliv. Rev. 61, 3–13.
Saulsbury, M.D., Heyliger, S.O., Wang, K., Round, D., 2008. Characterization of chlorpyrifos-induced apoptosis in placental cells. Toxicology 244, 98–110.
Schmidt, H.H., Gutsche, V., 2000. Analysis of the sales trend in plant protection products in the Federal Republic of Germany between 1980 and 1998 [in German]. Gesunde Pflanzen 52, 172–182.
Vähäkangas, K., Myllynen, P., 2009. Drug transporters in the human blood-placental barrier. Br. J. Pharmacol. 158, 665–678.
Wassermann, L., Halwachs, S., Lindner, S., Honscha, K., Honscha, W., 2013a. Determination of functional ABCG2 activity and assessment of drug-ABCG2 interactions in dairy animals using a novel MDCKII in vitro model. J. Pharm. Sci. 102, 772–784.
Wassermann, L., Halwachs, S., Baumann, D., Schaefer, I., Seibel, P., Honscha, W., 2013b. Assessment of ABCG2-mediated transport of xenobiotics across the blood-milk barrier of dairy animals using a new MDCKII in vitro model. Arch. Toxicol. 87, 1671–1682.